

# Fabrication of large Ti–6Al–4V structures by direct laser deposition

Qiu, Chunlei; Ravi, G.a.; Dance, Chris; Ranson, Andrew; Dilworth, Steve; Attallah, Moataz M.

DOI:

[10.1016/j.jallcom.2014.12.234](https://doi.org/10.1016/j.jallcom.2014.12.234)

License:

Other (please specify with Rights Statement)

*Document Version*

Peer reviewed version

*Citation for published version (Harvard):*

Qiu, C, Ravi, GA, Dance, C, Ranson, A, Dilworth, S & Attallah, MM 2015, 'Fabrication of large Ti–6Al–4V structures by direct laser deposition', *Journal of Alloys and Compounds*, vol. 629, pp. 351-361. <https://doi.org/10.1016/j.jallcom.2014.12.234>

[Link to publication on Research at Birmingham portal](#)

## **Publisher Rights Statement:**

NOTICE: this is the author's version of a work that was accepted for publication. Changes resulting from the publishing process, such as peer review, editing, corrections, structural formatting, and other quality control mechanisms may not be reflected in this document. Changes may have been made to this work since it was submitted for publication. A definitive version was subsequently published as C. Qiu, G.A. Ravi, C. Dance, A. Ranson, S. Dilworth, M.M. Attallah, Fabrication of large Ti-6Al-4V structures by direct laser deposition, *Journal of Alloys and Compounds* (2015), doi: <http://dx.doi.org/10.1016/j.jallcom.2014.12.234>

## **General rights**

Unless a licence is specified above, all rights (including copyright and moral rights) in this document are retained by the authors and/or the copyright holders. The express permission of the copyright holder must be obtained for any use of this material other than for purposes permitted by law.

- Users may freely distribute the URL that is used to identify this publication.
- Users may download and/or print one copy of the publication from the University of Birmingham research portal for the purpose of private study or non-commercial research.
- User may use extracts from the document in line with the concept of 'fair dealing' under the Copyright, Designs and Patents Act 1988 (?)
- Users may not further distribute the material nor use it for the purposes of commercial gain.

Where a licence is displayed above, please note the terms and conditions of the licence govern your use of this document.

When citing, please reference the published version.

## **Take down policy**

While the University of Birmingham exercises care and attention in making items available there are rare occasions when an item has been uploaded in error or has been deemed to be commercially or otherwise sensitive.

If you believe that this is the case for this document, please contact [UBIRA@lists.bham.ac.uk](mailto:UBIRA@lists.bham.ac.uk) providing details and we will remove access to the work immediately and investigate.

## Accepted Manuscript

Fabrication of large Ti-6Al-4V structures by direct laser deposition

Chunlei Qiu, G.A. Ravi, Chris Dance, Andrew Ranson, Steve Dilworth, Moataz M. Attallah

PII: S0925-8388(15)00029-8  
DOI: <http://dx.doi.org/10.1016/j.jallcom.2014.12.234>  
Reference: JALCOM 33027

To appear in: *Journal of Alloys and Compounds*

Received Date: 26 September 2014  
Revised Date: 22 November 2014  
Accepted Date: 25 December 2014



Please cite this article as: C. Qiu, G.A. Ravi, C. Dance, A. Ranson, S. Dilworth, M.M. Attallah, Fabrication of large Ti-6Al-4V structures by direct laser deposition, *Journal of Alloys and Compounds* (2015), doi: <http://dx.doi.org/10.1016/j.jallcom.2014.12.234>

This is a PDF file of an unedited manuscript that has been accepted for publication. As a service to our customers we are providing this early version of the manuscript. The manuscript will undergo copyediting, typesetting, and review of the resulting proof before it is published in its final form. Please note that during the production process errors may be discovered which could affect the content, and all legal disclaimers that apply to the journal pertain.

## Fabrication of large Ti-6Al-4V structures by direct laser deposition

Chunlei Qiu<sup>1</sup>, Ravi G. A<sup>1</sup>, Chris Dance<sup>2</sup>, Andrew Ranson<sup>2</sup>, Steve Dilworth<sup>2</sup>,  
Moataz M. Attallah<sup>1\*</sup>

<sup>1</sup>School of Metallurgy and Materials, University of Birmingham, Edgbaston, Birmingham B15 2TT, UK

<sup>2</sup>Integrated Operations, Manufacturing & Materials Engineering Department, BAE Systems Ltd, UK

### Abstract

Ti-6Al-4V samples have been prepared by direct laser deposition (DLD) using varied processing conditions. Some of the as-fabricated samples were stress-relieved or hot isostatically pressed (HIPed). The microstructures of all the samples were characterised using optical microscopy (OM), scanning electron microscopy (SEM) and X-ray diffraction (XRD) and the tensile properties assessed. It was found that a high laser power together with a reasonably low powder feeding rate was essential for achieving minimum porosity. The build height and geometrical integrity of samples was sensitive to the specified laser nozzle moving step along the build height direction (or Z step) with a too big Z step usually leading to a build height smaller than specified height (or under build) and a too small Z step to excessive building (or excess build). Particularly, scaling-up of samples requires a smaller Z step to obtain specified build height and geometry. The as-fabricated microstructure was characterised by columnar grains together with martensitic needle structure and a small fraction of  $\beta$  phase. This led generally to high tensile strengths but low elongations. The horizontally machined samples showed even lower elongation than vertically machined ones due to the presence of large lack-of-fusion pores at interlayer interfaces. HIPing effectively closed pores and fully transformed the martensites into lamellar  $\alpha+\beta$  phases, which considerably improved ductility but caused slight reduction in strength. With optimisation of processing conditions together with post-DLD HIPing, a couple of large spars with structural

integrity comparable to conventionally manufactured parts have been fabricated. Pronounced distortion was observed after unclamping of the as-fabricated structures. HIPing on the unclamped structures was found to significantly ease off the distortion. It is suggested that DLD plus HIPing is a feasible route for manufacturing high quality and high performance aerospace structures.

**Key words:** Titanium alloys; additive manufacturing; direct laser deposition; hot isostatic pressing; microstructure; fracture behaviour

\*Corresponding author: Tel: (+44) 121 414 7842; fax: (+44) 121 414 7890; e-mail address: [m.m.attallah@bham.ac.uk](mailto:m.m.attallah@bham.ac.uk) (M.M. Attallah)

## 1. Introduction

Direct laser deposition (DLD), also referred to as Laser-Engineered Net Shaping (or LENS), is one of the advanced additive manufacturing technologies that can be used to manufacture near net shape metallic components directly from CAD (computer aided design) models. Because it involves no thermomechanical processing and minimum machining, it can greatly reduce the buy-to-fly ratio and lead time for production, two factors which impact cost. Therefore, DLD is particularly attractive for the fabrication of titanium aerospace components and structures. Much of the focus of previous research has been on processing condition development based on small samples and on fabrication of small components for demonstration. Kobryn et al. [1, 2] studied the influence of laser processing conditions on porosity and microstructure development of Ti-6Al-4V and suggested that the porosity level decreased with increasing laser scanning speed and power level while the microstructure was generally dominated by columnar grains the width of which decreased with increasing scanning speed but increased with increasing incident energy density. Wu et al. [3-5] investigated the influence of laser power, scanning speed, and powder feed rate on grain structure and microstructural development and suggested that the size of columnar grains increased with decrease of laser scan speed while the size of the  $\alpha$  and  $\beta$  laths increases with increase of laser power and powder feed rate and decrease of scan speed. Lu et al. [6] studied the influence of post-DLD heat treatment on the laser fabricated Ti-6Al-4V microstructure and indicated that the annealing treatment has significant effect on the volume fraction, size and aspect ratio of primary  $\alpha$ , while the aging treatment mainly affects the volume fraction and aspect ratio of primary  $\alpha$  and the width and volume fraction of secondary  $\alpha$ . Kobryn and Semiatin [7] investigated the influence of HIPing on the microstructure and mechanical properties of DLDed samples and suggested that HIPing is effective in closing pores, improving ductility as well as mitigating mechanical anisotropy. This work increases the

understanding of the influence of processing condition on as-DLDED titanium samples and mechanical properties but most of this work has been done based on small samples (from several millimetres up to tens of millimetres) and mainly focused on microstructural development. The influence of processing condition and sample size (or scaling) on geometrical and structural integrity (porosity) of DLDED samples requires more investigation and better understanding.

In terms of fabrication of components by DLD, Wu and Mei [5] reported a number of small titanium components (from several centimetres up to tens of centimetres) with various geometries fabricated by DLD while Hedges and Calder [8] reported the application of DLD in manufacturing a series of near net shape small-sized aerospace and automobile components. This work demonstrates the capability of DLD process in manufacturing near net shape components. However, the report on manufacturing of large titanium components (at metre scale) using DLD is lacking and as a result the potential issues such as distortion and geometrical and quality control associated with scaling-up of samples or parts fabricated by DLD are not well understood. A couple of large titanium structures made by DLD were reported [9] but systematic study on the microstructure, mechanical properties, geometrical and structural integrity when samples are scaled up has not been reported.

On the other hand, it is widely recognised that quality control is critical for structures aimed for aerospace application. Defects such as porosity and distortion developed during DLD process together with mechanical anisotropy are some of the most common issues associated with DLD of Ti-6Al-4V. Kobryn et al. [1] suggested there are two types of pores in DLDED samples, gas pores which are generally spherical and lack-of-fusion pores which usually form at the interface between layers and show elongated or irregular-shaped morphology. The

latter was suspected to be one of the major causes for the anisotropy in yield strength of DLDED Ti-6Al-4V samples [7]. Thermal stress development and the resultant distortion of substrates and components during processing are particularly harmful for fabrication of large structures as the thermal stress could be enormous and the distortion of builds during processing could lead to inconsistent building during the following deposition and to eventual failure of builds. Normally, substrates need to be rigidly clamped prior to DLD when building large structures. In terms of study on distortion of substrate and component during DLD, so far, quite a few modelling has been developed to understand the thermal history, residual stress and distortion development during DLD of different shapes [10-13]. Experimentally, Moat et al [14] conducted residual stress measurement on some of the laser fabricated components and showed the stress distribution in the substrate and throughout the builds. Zhang et al [15] studied the influence of substrate preheating on the distortion level of thin substrates and parts during DLD and showed that substrate preheating could cause even more distortion during subsequent DLD processing and with increased preheating temperature, the distortion magnitude of the substrates and builds increased. Yu et al [16] suggested that laser deposition pattern could also affect the thermal distribution of builds and thus the distortion magnitude. Both the modelling and experimental work contributes to the understanding of stress and distortion development of laser fabricated samples and components and their influencing factors. Again, this work has been mainly focused on small (several centimetres) and simple shapes. More work is required to understand the distortion development during DLD of large structures and the influence of factors such as post-DLD heat treatment or HIPing.

In this paper, a parametric study has been performed on large Ti-6Al-4V T-section samples (tens of centimetres) to investigate the influence of processing conditions, such as laser power, powder feeding rate, and Z step geometrical and structural integrity of as-DLDED samples.

The scale effect, i.e., the influence of sample size (wall thickness and length) on geometrical integrity together with the influence of HIPing on geometrical and structural integrity, microstructure and mechanical properties was also investigated. Based on optimisation of processing conditions, attempts have been made to fabricate large (at metre scale) spars with different features.

## 2. Experimental

Gas atomised Ti-6Al-4V powder supplied by TLS Technik in the size range of  $75\mu\text{m}\sim 105\mu\text{m}$  was used. A 6.5-axis TRUMPF DLD (blown powder) system fitted with a 4kW disc laser and an automatic spot change collimator (from 0.2 to 6mm) has been used to fabricate samples. The setting up of this system is shown in Fig. 1(a) and the three-beam laser nozzle used is shown in Fig. 1(b). The spacing between the nozzle tip and the substrate ( $d_s$ ) was set up as 12mm which will give rise to a certain build layer thickness for a specific sample. When the  $d_s$  is higher than this value during building, a thinner build layer thickness and thus a lower build height would be seen. When  $d_s$  is smaller than 12mm during building, a thicker build layer thickness would be expected. The NC (numerical console) program was created from the CAD file using ALPHACAM Mill software provided by Planit CAD/CAM Software, UK. Laser energy was delivered through an optical fibre into the focal point that generates a melt pool on the surface of a metal base plate. Powder was fed using a SIEMENS powder feeder through a 3 beam nozzle by argon into the focal point. The desired spot size for the laser beam was achieved by varying the lens position automatically in the collimator.

The samples were deposited on Ti substrates with a thickness of 20mm in an argon atmosphere to limit oxidation. Prior to metal deposition, the oxygen level was brought down below 500ppm and the substrates were cleaned by laser scanning over the top surface at



1000W and 800mm/min. The oxygen level of the material before and after processing was also measured using a LECO TC436AR ANALYSER. To find out optimum processing conditions, parametric study was conducted on a particular T-section sample, the geometry of which is shown in Fig. 2. A wide range of laser powers (800-1500W), laser scanning speeds (600mm/s-1000mm/s), powder feeding rates (6-16g/min) and Z steps (0.5-1.5mm) have been investigated. The initial selection of process conditions started with geometrical check of as-fabricated T-section samples. Those processing conditions that gave rise to required geometry and build height would be considered as good ones as shown in Fig. 3(a) and further characterisation (porosity, microstructure) would be focused on these samples whereas the conditions leading to under building that is usually associated with undulated surfaces (see Fig. 3(b)) would be considered as bad conditions. Excessive/excess building could also happen. It does not affect the geometry considerably except that the build height is higher than specified value and it still gives flat top build surface which is good. The problem with excessive building is that it decreases the spacing ( $d_s$ , as shown in Fig. 1(a)) between nozzle tip and the top surface of a build during processing, which would allow melted or partially melted powder particles to bounce more easily back into nozzle holes and cause clogging of the holes. This would in turn affect the build quality. Therefore, processing conditions leading to too much excess build will be considered as bad conditions as well. T-section samples with different scales and dimensions were also prepared under an identical processing condition to investigate the influence of scaling-up of samples on geometrical integrity.

Metallographic specimens were prepared from the T-sections with good geometrical integrity using conventional methods and examined using OM and SEM in a JEOL 7000 FEG-SEM microscope to reveal the pore size, distribution and morphology. To show porosity distribution over a large area of the samples, tens of OM frames have been stitched to

develop a whole picture of a single section. Porosity level was evaluated by measuring the area fraction ( $A_f$ ) of pores using Image J software.

HIPing was also performed on some as-DLDed samples to study its influence on structural integrity, microstructure and mechanical properties. HIPing was conducted at a standard condition of 920°C/100MPa/4h followed by furnace cooling (with cooling rate of around 5°C/min). Some as-DLDed samples were also annealed at 700°C for 4hours to relieve residual stress. The as-fabricated, DLDed+annealed and DLDed+HIPed samples were ground, polished and examined by XRD. They were also etched in an etchant containing 50 ml distilled water, 25 ml HNO<sub>3</sub> and 5 ml HF for microstructural characterisation using OM and SEM.

Tensile tests were performed at room temperature using a computer-controlled electric screw driven Zwick/Z100 tensile testing machine on both as-DLDed and DLDed+HIPed samples. Cylindrical specimens were machined along both vertical and horizontal directions of T-section samples for tensile testing. The samples were tested along their axis and the tests were conducted under strain control mode with a strain rate of  $1.0 \times 10^{-3} \text{ s}^{-1}$ . Tensile fracture surfaces were examined using SEM.

### **3. Results**

#### **3.1 Influence of processing condition on geometrical and structural integrity**

Table 1 shows several processing conditions that enable the fabrication of T-sections with required geometry and build height. It was found that the build height and geometry are particularly sensitive to Z step, with its change at a level of several tens of microns from the

values listed in the table being able to lead to pronounced under build or excess build after tens of layers' deposition. This would be further demonstrated in the following section.

Fig. 4 shows the porosity distribution in the samples fabricated using the processing condition listed in Table 1. It can be seen that a high laser power plus a high powder feeding rate (Process 1, Fig. 4(a)) leads to the development of quite a few large irregular-shaped pores (at millimetre scale). When the laser power and powder feeding rate were decreased to a much lower level (Process 2, Fig. 4(b)), the pore width is greatly reduced but considerable flat pores are developed. These pores are usually associated with incompletely melted powder particles (Fig. 4(c) and (d)) and are believed to be due to lack of fusion or incomplete remelting of previous layers. However, it is noted that a high laser power combined with low powder feed rates (Process 3 in Fig. 4(e) and Process 4 in Fig. 4(f)) could significantly reduce the porosity level. The results suggest that a combination of a sufficiently high laser power and a reasonably low powder feed rate and Z step is essential for achieving good structural integrity.

HIPing was also conducted on some of the as-fabricated samples that contain considerable pores to investigate its influence on structural integrity. The results are shown in Fig. 5. It is obvious that HIPing has effectively closed the large irregular-shaped or flat pores. Throughout the DLDed+HIPed samples, some traces that clearly show the collapse of pores by bridging could be observed (Fig. 5(c) and (d)).

### **3.2 Influence of sample size and Z step on build height and geometrical integrity**

Fig. 6 and Table 2 show the geometry and build status of T-sections with varied wall lengths or thicknesses fabricated under the same processing condition (i.e. with identical laser power, scanning speed and powder flow rate) but with different Z steps. It can be seen that with varied sample sizes, selection of a proper Z step is essential for achieving specified build

height. Actually, the use of a too big Z step for a specific sample size usually leads to under build and undulated surface, as shown in Fig. 6 (a),(c),(e) and (g). The specified build height could be achieved by reducing Z step to a certain level (see Fig. 6(b),(d),(f),(h)). Too small Z step would lead to excess build and clogging of nozzle as described above. Also, it is noted that using the Z step that has given rise to required build height for the sample with thinner walls resulted in under building for the samples with thicker walls (see Fig. 6 (b) and (c)). To achieve desired build height for the T-sections with thicker walls, a smaller Z step is needed (see Fig. 6(d)). In the comparison between the other two groups of samples (Fig. 6(e-f) and (g-h)) where the wall thicknesses are the same but the lengths of the webs are different, similarly, a smaller Z step is required to obtain desired build height for the samples with longer webs (see Fig. 6(f) and (h)). That the build height and geometrical integrity change with sample wall thickness and length seems to suggest that there is a certain dependence of material contraction on sample size during solidification and cooling processes. The bigger samples tend to experience more material contraction than smaller ones as they usually develop into under build when using identical processing conditions that have been used to fabricate smaller samples.

### 3.3 Microstructure and mechanical properties

Fig. 7 show the typical microstructure of as-DLDed and DLDed+HIPed samples. It can be seen that the as-fabricated sample is generally dominated by columnar grains and martensitic needle structure. The columnar grains seem to have grown parallel to the heat loss directions with grains in the middle generally growing along build height direction or Z direction where heat mainly dissipates via substrate while the grains in the peripheral regions extending in a slant angle relative to the Z direction where heat lost via both substrate and radiation. After HIPing, the needle structure is fully transformed into lamellar  $\alpha+\beta$  structure. XRD analysis

shown in Fig. 8 suggests that there is a certain amount of  $\beta$  phase present throughout the as-fabricated samples. Annealing at 700°C does not seem to cause significant change in microstructure although it does lead to stress relieving given that no distortion could be observed when the samples were detached. After HIPing, the samples tend to show the strongest  $\beta$  peak in the XRD spectra suggesting that the volume fraction of  $\beta$  phase may have been increased by HIPing, which is consistent with SEM observation.

Oxygen analysis was also conducted on different regions of a T-section sample. The results are shown in Fig. 9, which suggests that the oxygen pickup is generally limited during DLD thanks to the argon protective atmosphere. Nevertheless, the bottom region tends to have the maximum oxygen pickup while the top region has only a marginal pickup.

Fig. 10 and Table 3 show the tensile testing results of as-DLDed and DLDed+HIPed samples (produced using Process 2). It can be seen that the as-DLDed samples show generally high 0.2% yield strengths (YS) and ultimate tensile strengths (UTS) but low elongations (<10%). Their strengths are even higher than their forged and heat treated counterparts. The high strengths are believed to be associated with the fine microstructure and residual stress remained in the as-DLDed samples. The horizontal specimens tend to show better elongation than their vertical counterparts, resulting in anisotropy in ductility. Similar anisotropy was also observed in previous work [7]. HIPing considerably improves the elongation and fully eliminates the anisotropy in elongation but leads to a reduction in 0.2% YS and UTS. This makes the strengths of DLDed+HIPed samples slightly lower than their forged and heat treated counterparts.

To better understand the tensile behaviour of the samples investigated, the fracture surfaces of the tested specimens were further examined and the results are shown in Fig. 11 and Fig. 12. It is obvious that the as-fabricated specimens taken out along different directions from T-

section samples show very different fracture features. The vertical samples show quite a few large opened-up pores on their fracture surfaces. These pores show smooth surfaces decorated with un-melted or partially melted powder particles suggesting that this layer was not completely remelted during the subsequent building. This kind of pores is known as lack-of-fusion pores and is extremely harmful for mechanical properties [7]. The horizontal specimens, however, show closed pores or seams that are normal to the fracture surface. The difference in the fracture feature between the samples machined from different directions is believed to be due to the difference in the loading direction relative to the orientation of the pores that are usually located at inter-layer boundaries and show flat or angular morphologies as described above (see Fig. 4). Thus, in the case of as-DLDed vertical samples, the loading direction is normal to the orientation of pores (see Fig. 11(g)) and thus the pores tend to be torn apart whereas for the as-DLDed horizontal samples, the loading is nearly parallel to the flat pores imposing compression stress upon the pores locally, which helps seal and close the pores. In contrast to as-DLDed samples, the DLDed+HIPed samples, in spite of different orientations, all show no obvious pores on the fracture surfaces and instead exhibit a fairly ductile fracture surface characterised by massive dimples, as shown in Fig. 12.

### **3.4 Fabrication of large aerospace structures**

With optimisation of processing conditions, two large spars containing walls of different thicknesses and orientations have been fabricated (see Fig. 13). After unclamping these structures were considerably distorted as shown in Fig. 14(a-c). HIPing was carried out to relieve residual stress and restore the shape from distortion after unclamping; the results are shown in Fig. 14(d-f). Obviously, with HIPing, the structure has experienced a good recovery from distortion; only a tiny lifting still remains at two ends. The DLDed+HIPed structures show no obvious defects on the surfaces after machining, suggesting that a good structural

integrity has been achieved. The quality of the machined structure is believed to be comparable to its conventionally manufactured (i.e., cast+forged) counterpart.

#### 4. Discussion

The results have demonstrated that the build height and geometry of as-DLDED samples and structures could be affected by many factors such as laser power, powder flow rate, Z step and even sample size. It was found that a high laser power together with a reasonably low powder flow rate is essential for structural integrity, as shown in Fig.3. This is probably due to that a good combination of laser power and powder flow rate would guarantee sufficient melting of the captured powder and thus avoid the development of lack-of-fusion pores. The build height and geometrical integrity is also found to be sensitive to specified Z step. Ideally, the actual building layer thickness should match the specified Z step so that the spacing between the nozzle tip and the build surface ( $d_s$  in Fig. 1(a)) would be kept constant and the building will be consistent throughout the whole build and give rise to specified build height and geometry. Any deviation of the actual building layer thickness from Z step would lead to variation in  $d_s$  and thus would cause the change of powder spreading and capture rate and consequently change in actual layer thickness. This could further expand the mismatch between actual layer thickness and Z step as the building proceeds and eventually lead to pronounced under build or excess build. Moreover, the dependence of build height and geometrical integrity on sample size (wall thickness and length) is also recognized in the current work. The dependence is believed to be due to varied extents of material contraction with sample sizes during solidification and cooling. The bigger samples tend to experience more material contraction than smaller ones as they usually develop into under build when using the same processing condition and Z step that are good for building smaller samples. With more pronounced material contraction, the actual build layer thickness for larger

samples would be lower than the specified layer thickness which is the Z step. As a result, the gap between the nozzle tip and the build surface,  $d_s$ , would be increasingly widened layer after layer and less material will be captured or deposited onto the top surfaces, eventually leading to under build. Only by reducing Z step to match the actual build layer thickness for larger samples could a constant  $d_s$  be maintained and consistent building guaranteed. The sample size dependence of build height together with the fact that it is usually a time-consuming process to identify a right Z step for DLD of a specific geometry makes it highly necessary to introduce an in-situ monitoring and sensing system so that the real-time actual building layer thickness and build height could be understood. The automation of the DLD system in dealing with feedback and new building information should also be improved so that the Z step could be adjusted in a timely manner to correct any deviation of build height from specified value caused by any imprecise deposition on previous layers. In short, a good processing condition together with a proper Z step is essential for successful building of large structures by DLD.

Another interesting phenomenon observed in the current study is the development of anisotropy in tensile properties due to the presence of irregular-shaped or flat pores. These pores are usually planar and associated with some un-melted or incompletely melted powder particles as shown in Fig. 11, suggesting that their formation was due to incomplete remelting of the layer surface and incomplete melting of powder particles that fell onto those sites. These pores are extremely harmful for mechanical properties especially when there is tensile stress upon them. They could act as favourable crack initiation and propagation sites and cause early failure of the samples. However, when they are under compression stress condition they would tend to be closed but still could act as crack initiation sites. The presence of this type of pores and the consequent anisotropy in mechanical properties need to be avoided when it comes to critical application. HIPing has been proven to be effective in



closing and healing these pores and in eliminating mechanical anisotropy. HIPing was also surprisingly found to be an effective method to recover structure shapes from significant distortion induced by the relief of enormous residual stress after unclamping. The reason for this is believed to be due to the heavy weight of the spar itself which brought the spar back towards flat especially when it is hot and softened during HIPing. Based on the current work, it is suggested that a DLD+HIPing process would be a feasible route for manufacturing high quality and high performance components and structures.

## 5. Conclusions

- Selection of proper processing parameters particularly laser power, powder feeding rate and Z step is essential for successful building of samples and structures
- With optimised processing condition, large structures could be fabricated by DLD process
- The as-fabricated samples were dominated by columnar grains and martensites and show generally superior tensile strengths but low elongations
- The presence of planar pores due to incomplete remelting of previous layer caused pronounced anisotropy in ductility
- HIPing is effective in closing planar pores and is able to completely transform martensitic structure into  $\alpha+\beta$  lamellar structure, which led to improvement of ductility and to the elimination of mechanical anisotropy
- HIPing is also effective in recovering structure shape from considerable distortion induced by stress relief due to unclamping.

## Acknowledgements

The work shown in this paper was part of a SAMULET-4 project (Strategic Affordable Manufacturing in the UK through Leading Environmental Technologies) and was financially sponsored by Technology Strategy Board (TSB), UK. The authors are grateful to Dr. Stephen McCaine, Dr. Kiran Gulia and Mr. Mick Wickins for their help and assistance in this project.

## References

- [1] P.A. Kobryn, E.H. Moore, S.L. Semiatin, Microstructure and texture evolution during solidification processing of Ti–6Al–4V, *J. Mater. Proc. Tech.* 135(2003) 330-339
- [2] P.A. Kobryn, E.H. Moore, S.L. Semiatin, The effect of laser power and traverse speed on microstructure, porosity, and build height in laser-deposited Ti-6Al-4V. *Scripta. Mater.* 43(2000)299-305
- [3] X. Wu, J. Liang, J. Mei, C. Mitchell, P.S. Goodwin, W. Voice, Microstructures of laser-deposited Ti–6Al–4V, *Mater. Des.* 25(2004)137-144
- [4] X. Wu, A review of laser fabrication of metallic engineering components and of materials, *Mater.Sci.Tech.* 23(2007)631-640
- [5] X. Wu, J. Mei, Near net shape manufacturing of components using direct laser fabrication technology, *J. Mater. Proc. Tech.* 135(2003)266–270
- [6] Y. Lu, H.B. Tang, Y.L. Fang, D. Liu, H.M. Wang, Microstructure evolution of sub-critical annealed laser deposited Ti–6Al–4V alloy, *Mater. Des.* 37(2012)56-63.
- [7] P.A. Kobryn, S.L. Semiatin. Mechanical Properties of Laser-Deposited Ti-6Al-4V. *Solid Freeform Fabrication Symposium Proceedings, Austin, 2001, 179-186*
- [8] M. Hedges, N. Calder, 2006. Near net shape rapid manufacture & repair by LENS. The report could be accessed at: [www.dtic.mil/cgi-bin/GetTRDoc?AD=ADA524690](http://www.dtic.mil/cgi-bin/GetTRDoc?AD=ADA524690)
- [9] 16th China International High-Tech Expo, Beijing, 2013. The report on the world's largest titanium aircraft critical component produced using 3D laser direct manufacturing technology could be accessed at: <http://www.3ders.org/articles/20130529-china-shows-off-world-largest-3d-printed-titanium-fighter-component.html>
- [10] S. Marimuthu, D. Clark, J. Allen, A.M. Kamara, P. Mativenga, L. Li, R. Scudamore. *Proceedings of the Institution of Mechanical Engineers, Part C: J. Mech. Eng. Sci.* 0(2013)1–13
- [11] M. Labudovic, D. Hu, R. Kovacevic, A three dimensional model for direct laser metal powder deposition and rapid prototyping, *J. Mater. Sci.* 38(2003)35– 49
- [12] S. Zekovic, R. Dwivedi, R. Kovacevic. Thermo-structural Finite Element Analysis of Direct Laser Metal Deposited Thin-Walled Structures. *Proceedings of the Solid Freeform Fabrication Symposium, Austin, Texas, 2005, pp. 338-355.*

- [13] H. Liu, T.E. Sparks, F.W. Liou, D.M. Dietrich. Numerical Analysis of Thermal Stress and Deformation in Multi-Layer Laser Metal Deposition Processes. Proceedings of the Solid Freeform Fabrication Symposium, Austin, Texas, 2014, pp. 577-591.
- [14] R.J. Moat, A.J. Pinkerton, L. Li, P.J. Withers, M. Preuss, Residual stresses in laser direct metal deposited Waspaloy, *Mater. Sci. Eng. A*, 528(2011) 2288–2298.
- [15] J. Yu, X. Lin, L.Ma, J.J. Wang, X.L. Fu, J. Chen, W.D. Huang, Influence of laser deposition patterns on part distortion, interior quality and mechanical properties by laser solid forming (LSF), *Mater. Sci. Eng. A*. 528 (2011)1094–1104
- [16] K. Zhang, S.J. Wang, W.J. Liu, R.S. Long, Effects of substrate preheating on the thin-wall part built by laser metal deposition shaping, *Appl. Surf. Sci.* 317(2014)839–855
- [17] G.A. Ravi, X.J. Hao, N. Wain, X. Wu, M.M. Attallah, Direct laser fabrication of three dimensional components using SC420 stainless steel, *Mater. Des.* 47(2013)731-736
- [18] Z.W. Wu, C.L. Qiu, V. Venkatesh, H.L. Fraser, R.E.A. Williams, G.B. Viswanathan, M. Thomas, S. Nag, R. Banerjee, M. H. Loretto, *Metall. Mater. Trans. A*. 44(2013)1706-1713

## Figure captions

Fig. 1 (a) Schematic illustration of the setting up of the Trumpf DLD system,  $d_s$  is the spacing between laser nozzle tip and build surface [17]; (b) a photo showing the 3-beam laser nozzle.

Fig. 2 CAD model of a T-section,  $a$  and  $b$  represent the specified lengths of the two webs of a T-section and  $c$  and  $h$  represent the specified width and height of the walls, respectively. For parametric study,  $a*b*c*h = 111*75*16*70\text{mm}$

Fig. 3 As-fabricated T-sections, (a) build with required geometry and height; (b) build with under building and undulated surface.

Fig. 4 OM X-Z sectional images showing porosity distribution and level for (a) Process 1,  $A_f = 0.36\%$ ; (b) Process 2,  $A_f = 0.177\%$ ; (c-d) Process 2; (e) Process 3,  $A_f = 0.013\%$ ; (f) Process 4,  $A_f = 0.076\%$ .

Fig. 5 OM X-Z sectional images of as-DLDed builds (a) before and (b) after HIPing; (c) and (d) SEM images of closed or bridged pores in DLDed+HIPed samples.

Fig. 6 T-sections with varied dimensions fabricated under an identical processing condition but with varied Z steps: (a)-(b)  $a*b*c = 111*75*10\text{mm}$ , Z step in (a) is ( $Z_o+0.133$ ) and in (b) ( $Z_o+0.12$ ). (c)-(d)  $a*b*c = 111*75*22\text{mm}$ , Z step in (c) is ( $Z_o+0.091$ ) and in (d)  $Z_o$ . (e)-(f)  $a*b*c = 160*140*18\text{mm}$ , Z step in (e) is ( $Z_o+0.12$ ) and in (f) ( $Z_o+0.085$ ). (g)-(h)  $a*b*c = 328*85*18\text{mm}$  Z step in (g) is ( $Z_o+0.085$ ) and in (h) ( $Z_o+0.063$ ). The specified build height  $h$  for all the T-sections is 70mm.

Fig. 7 (a)-(c) OM X-Z sectional micrographs showing grain structure in as-DLDed samples; (d) and (e) back scattered electron SEM micrographs showing microstructure of as-DLDed and DLDed+HIPed samples, respectively. The arrows show the grain growth directions in different regions of the samples.

Fig. 8 XRD results of as-DLDed samples (from bottom region up to top region of a T-section), DLDed+annealed sample and DLDed+HIPed sample.

Fig. 9 Oxygen level in as-received powder and as-fabricated samples (from bottom region up to top region).

Fig. 10 (a) Schematic illustration of vertical and horizontal tensile specimens; (b) tensile stress-strain curves of vertical samples before and after HIPing; (c) tensile stress-strain curves of horizontal samples before and after HIPing.

Fig. 11 SEM micrographs of the fracture surfaces of as-DLDed samples, (a) and (b) vertical samples; (c) and (d) horizontal samples; (g) and (h) schematic illustration of tensile loading direction relative to the orientations of the angular or flat interlayer pores in vertical and horizontal samples, respectively.

Fig. 12 SEM micrographs of the fracture surfaces of DLDed+HIPed samples, (a)-(b) vertical sample; (c)-(d) horizontal sample

Fig. 13 (a) as-fabricated Spar 1 with a length of 1.1m and a wall thickness of 20mm; (b) as-fabricated Spar 2 with a length of 1.1m and varied wall thicknesses (8~16mm) and orientations

Fig. 14 (a)-(c) as-fabricated Spar 1 after unclamping showing considerable distortion; (d)-(f) unclamped Spar 1 after HIPing showing recovery from distortion; (g) build quality of Spar 1 after machining

ACCEPTED MANUSCRIPT

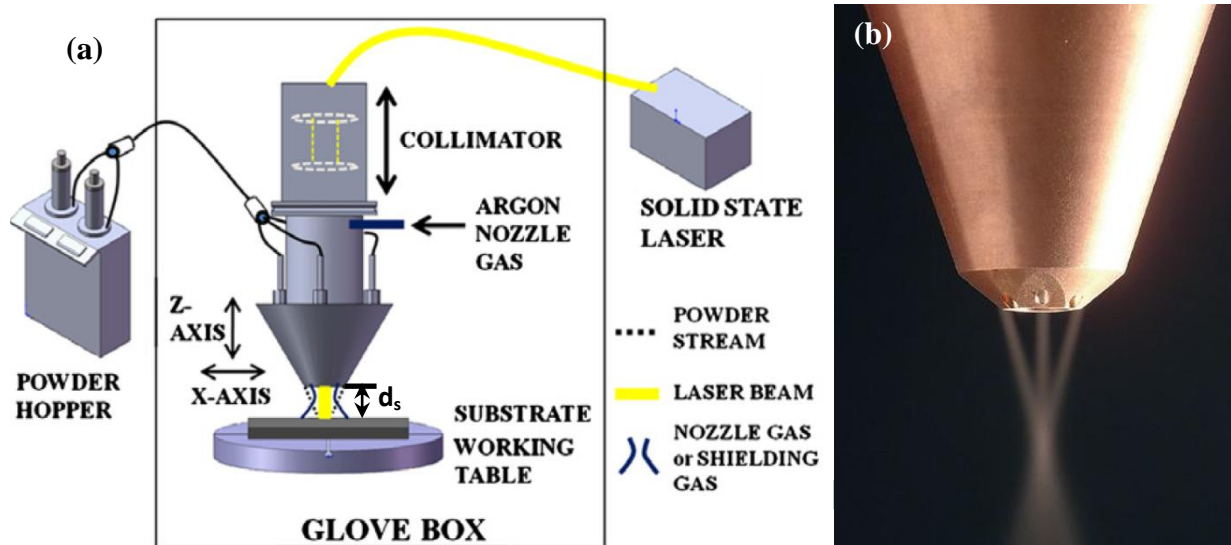
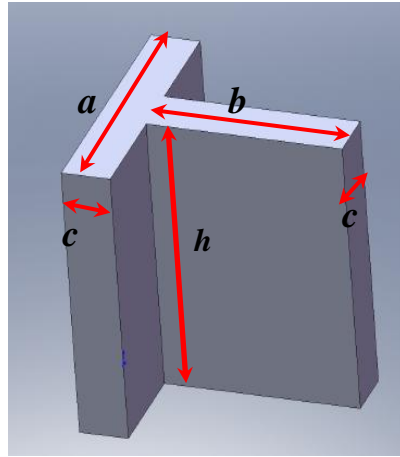


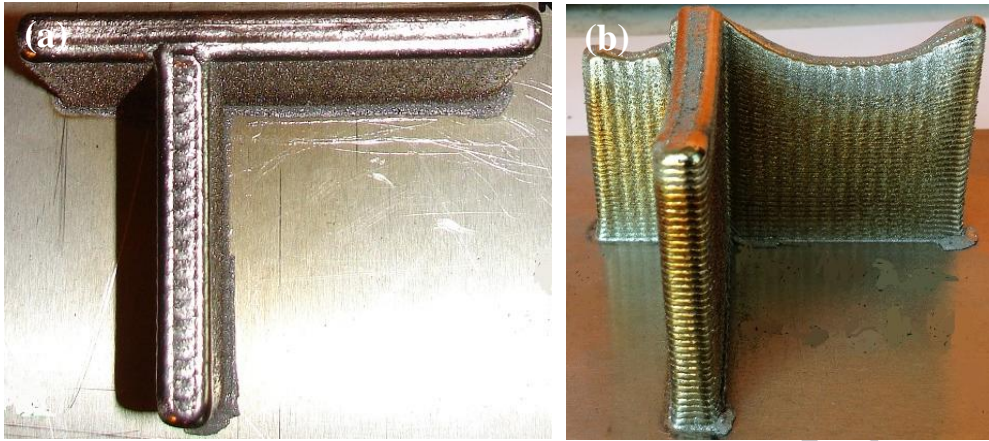
Fig. 1



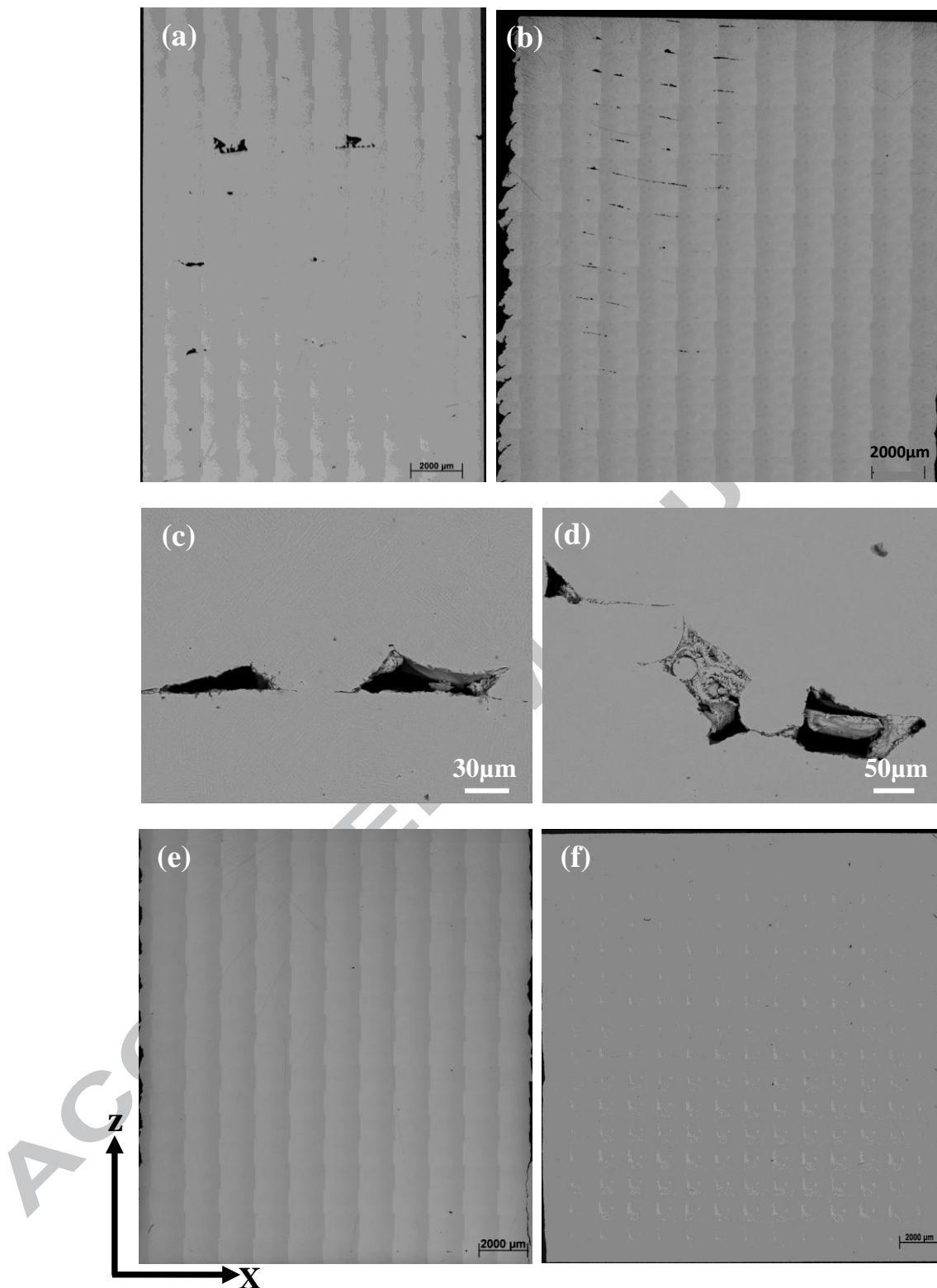
**Fig. 2**

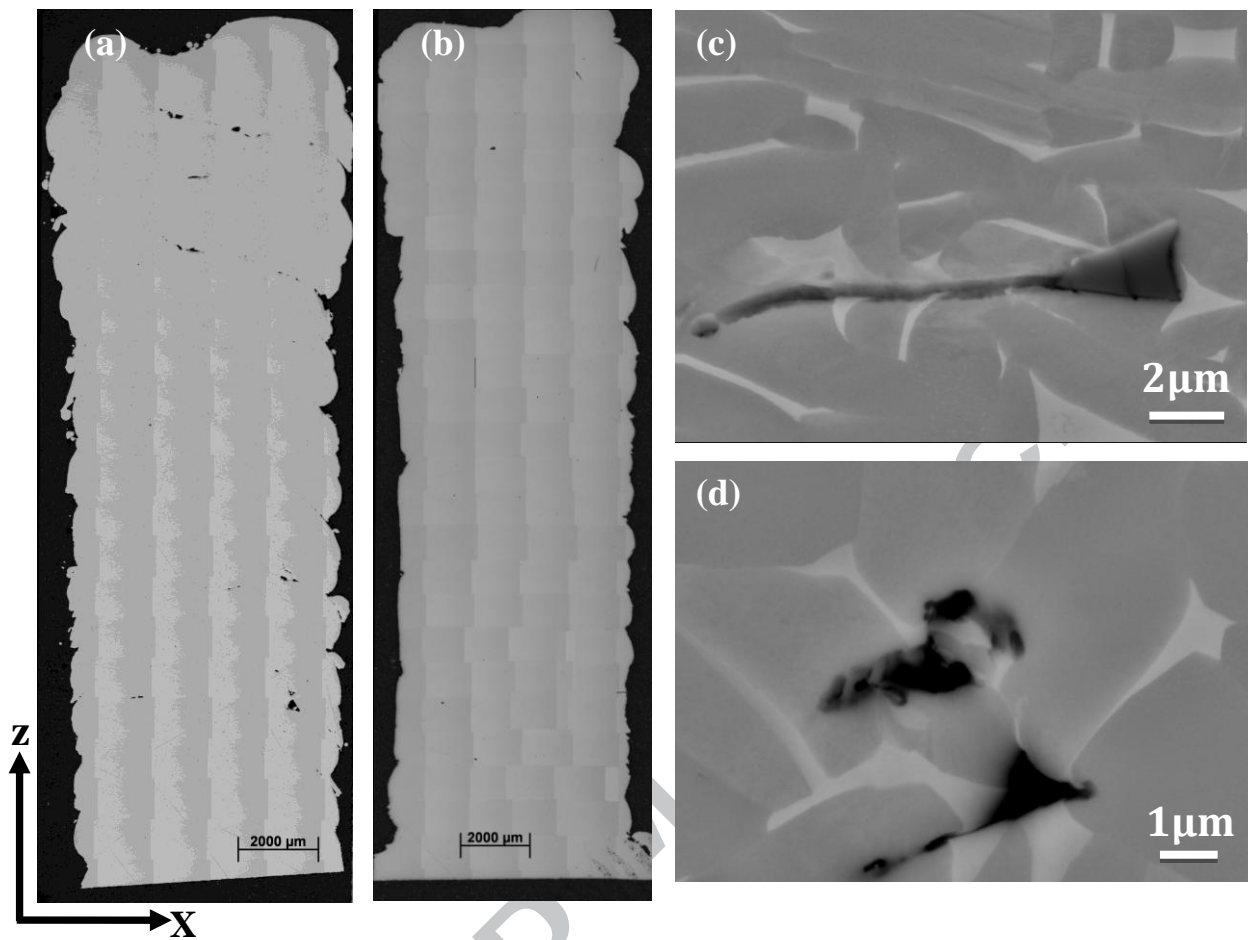
ACCEPTED MANUSCRIPT

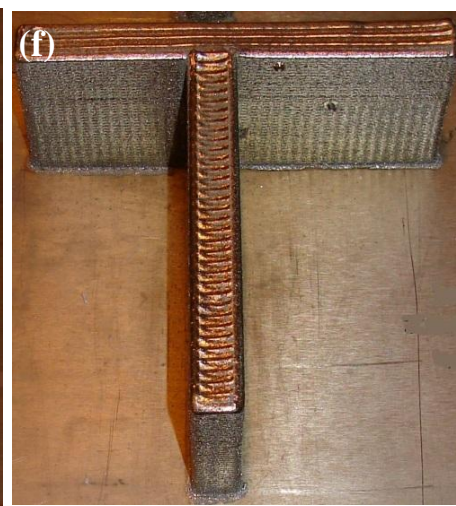
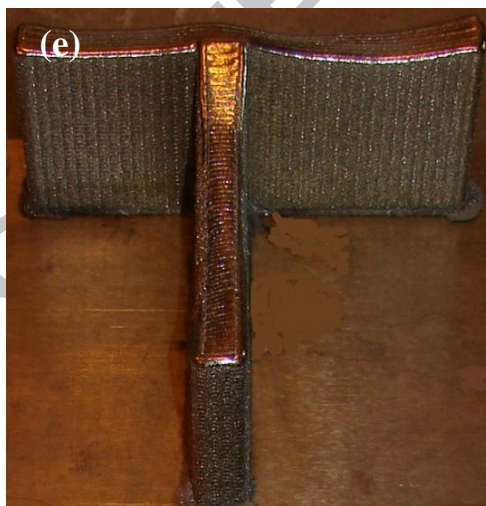
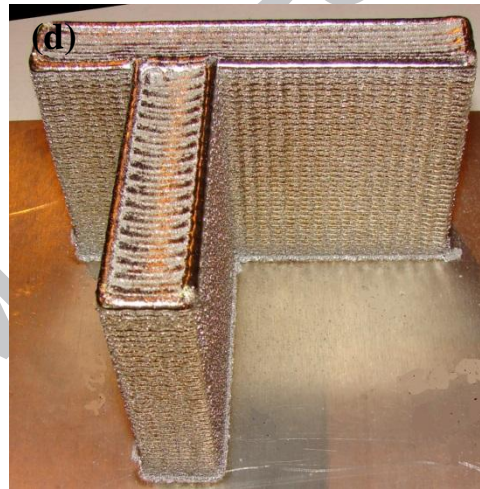
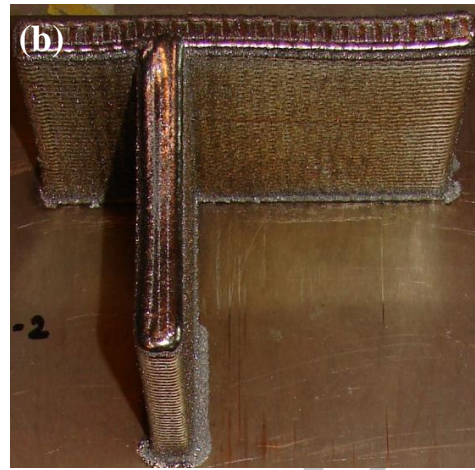




**Fig. 3**

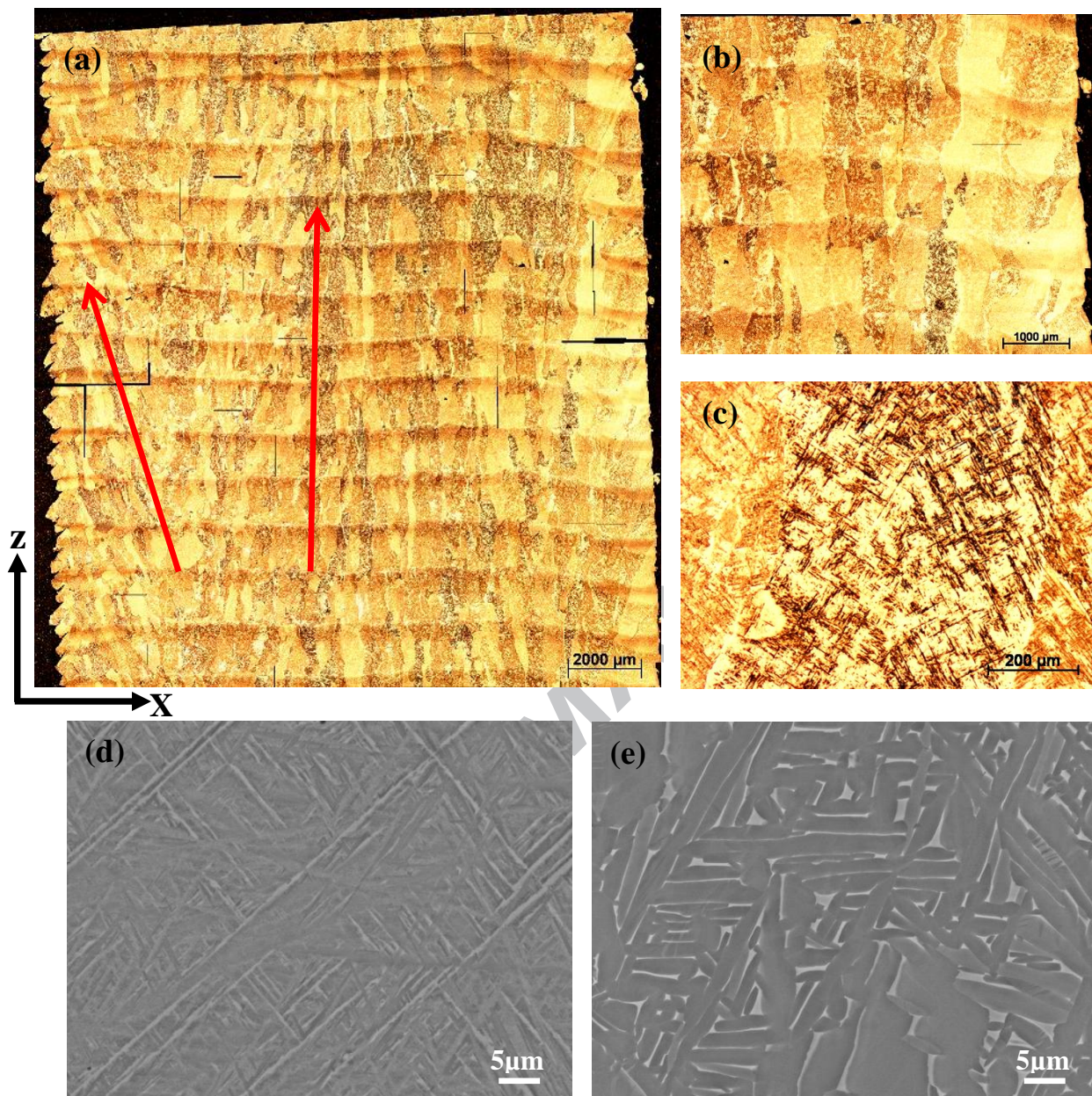
**Fig. 4**

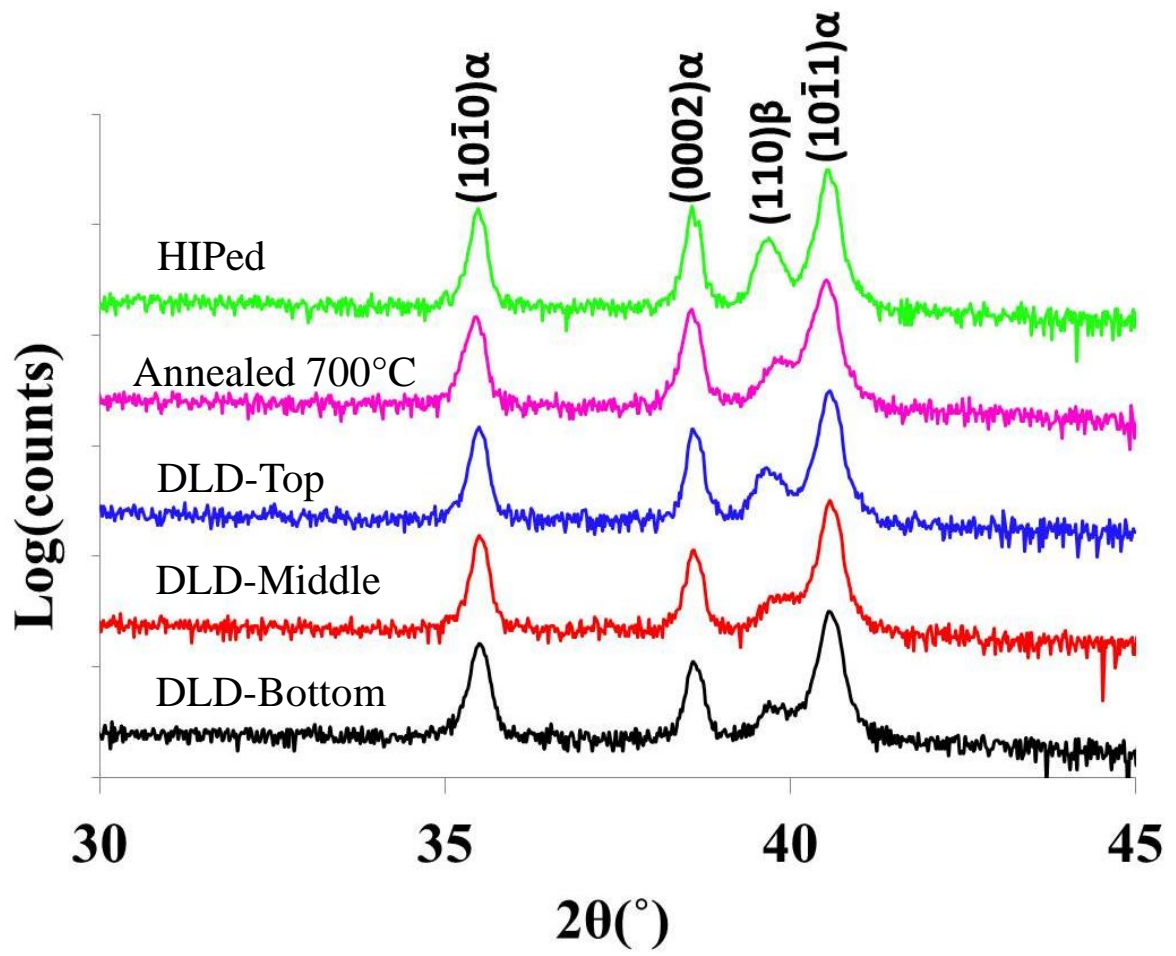
**Fig. 5**

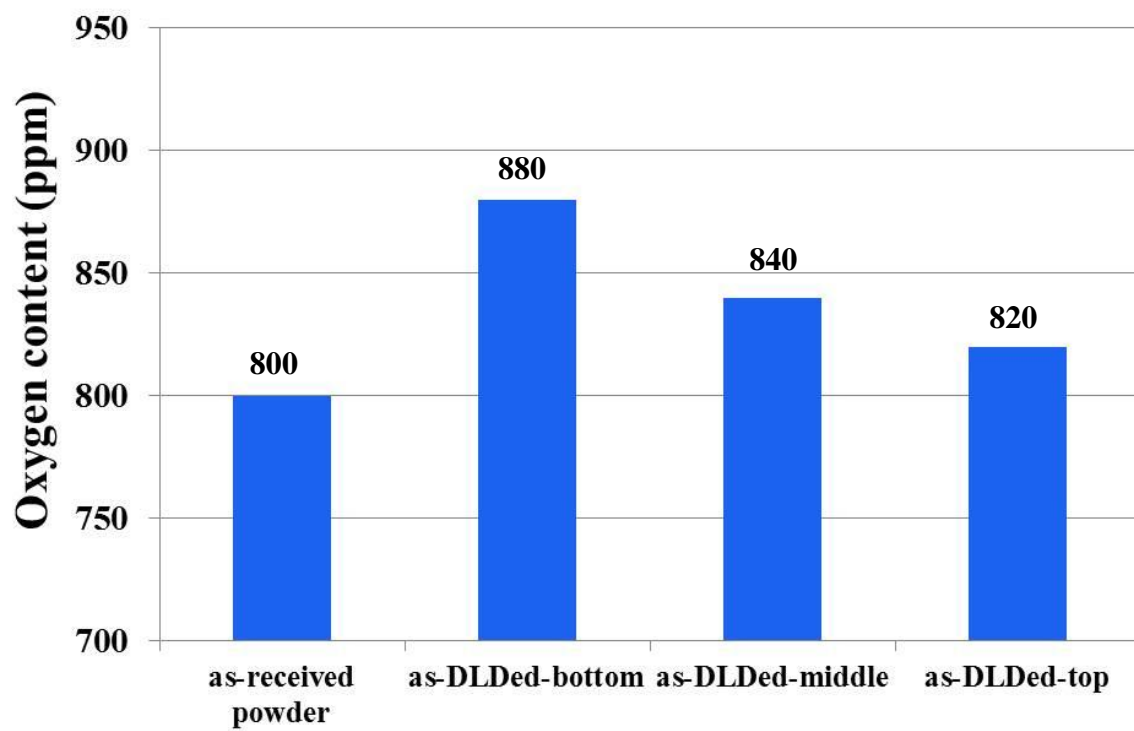




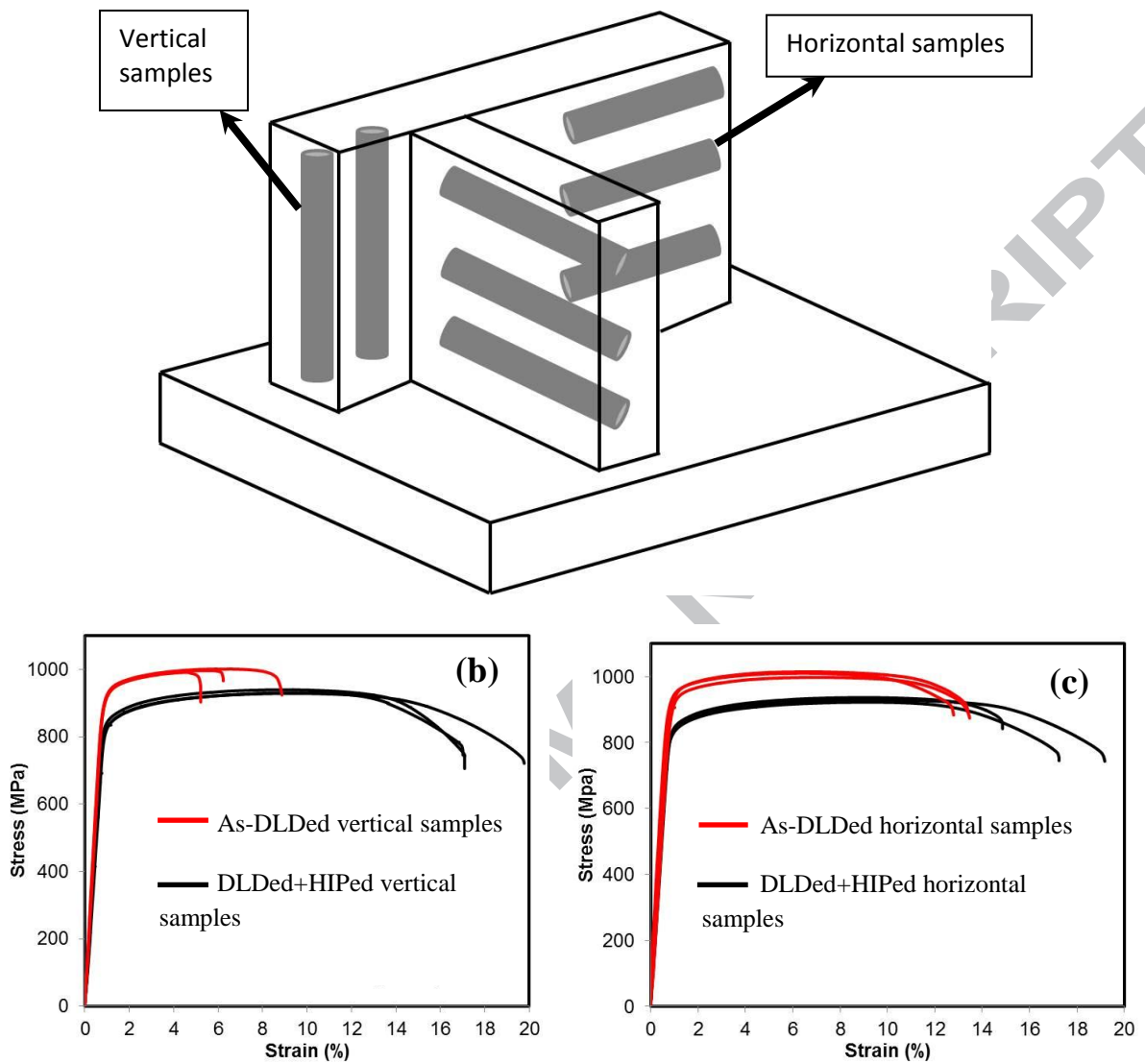
**Fig. 6**

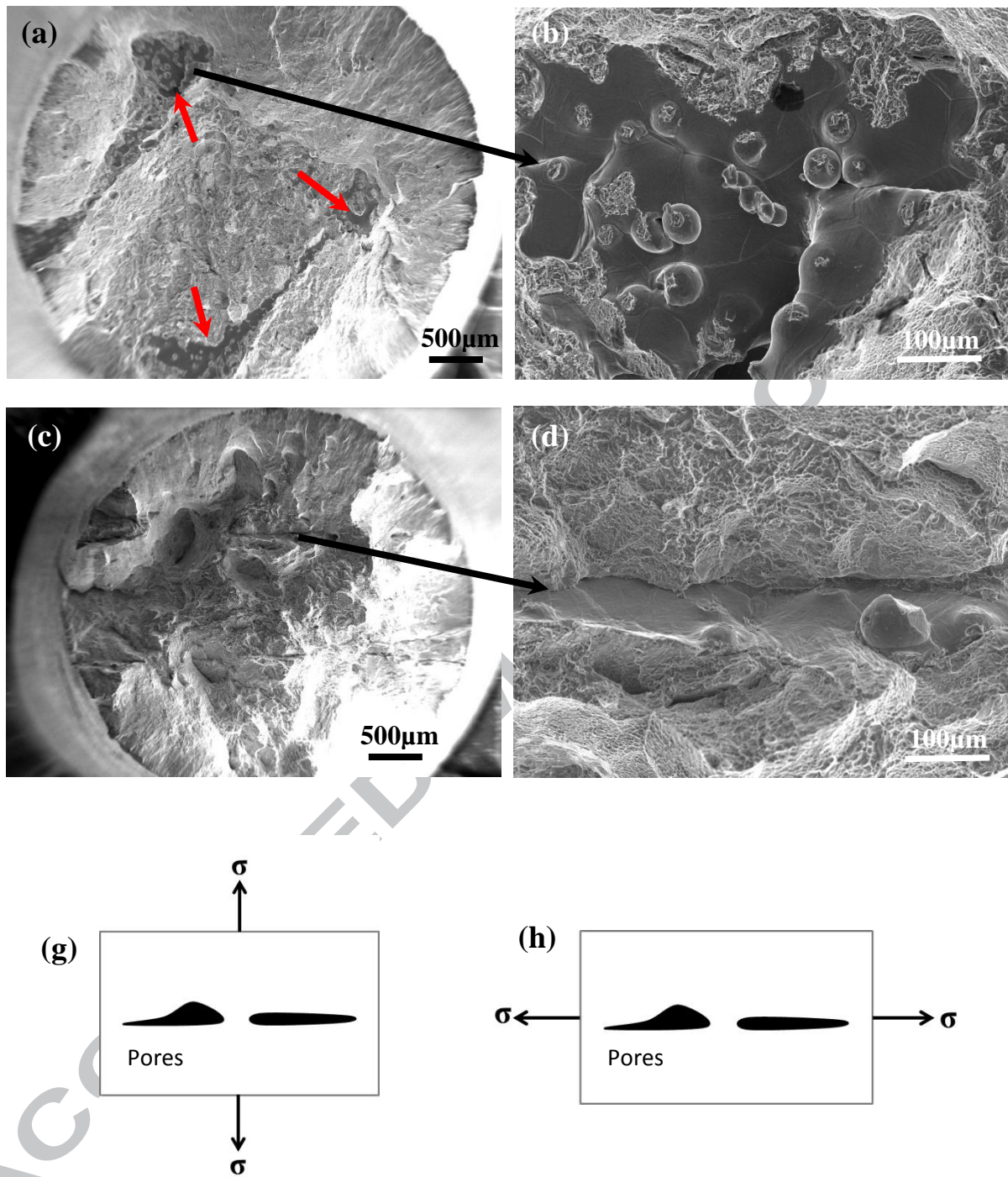
**Fig. 7**

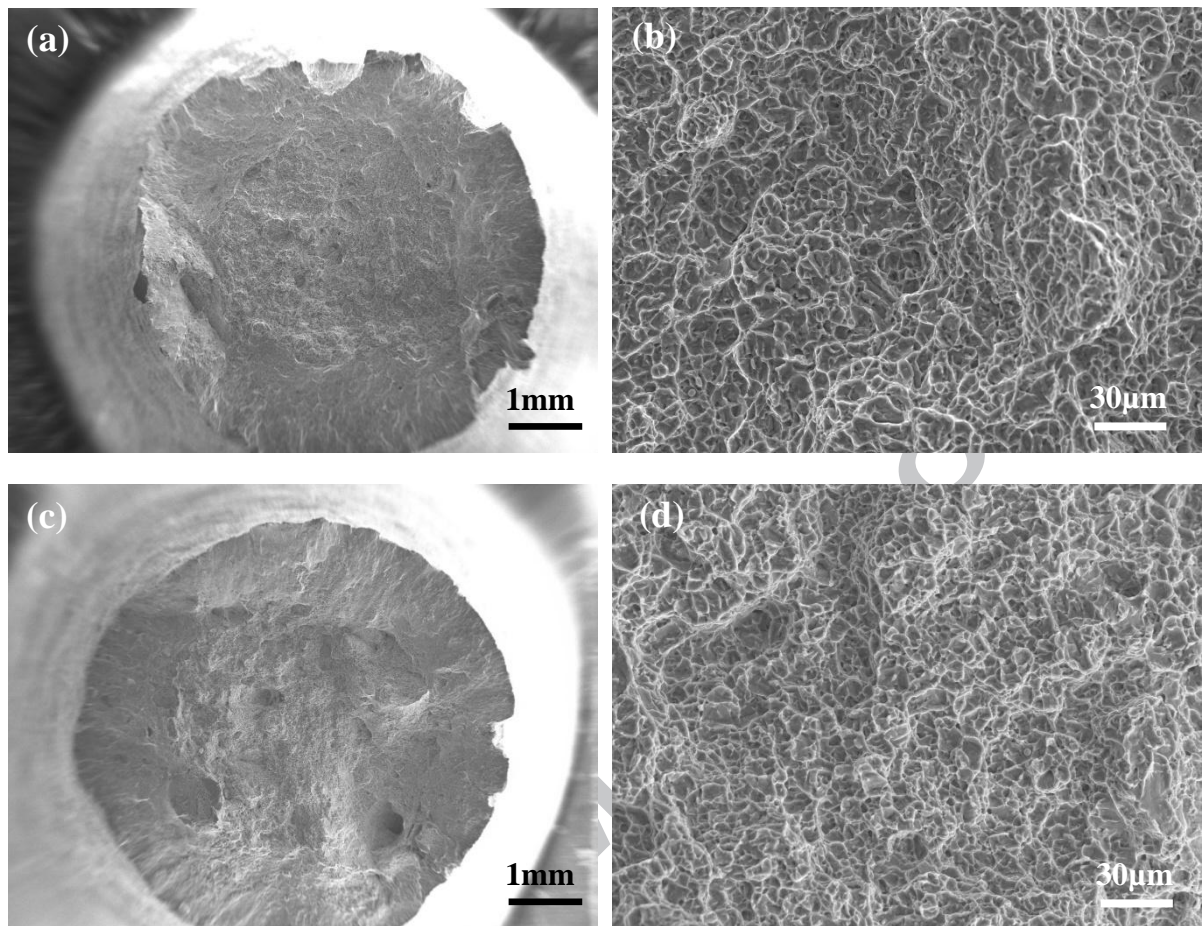
**Fig. 8**

**Fig. 9**



**Fig. 10**

**Fig. 11**

**Fig. 12**

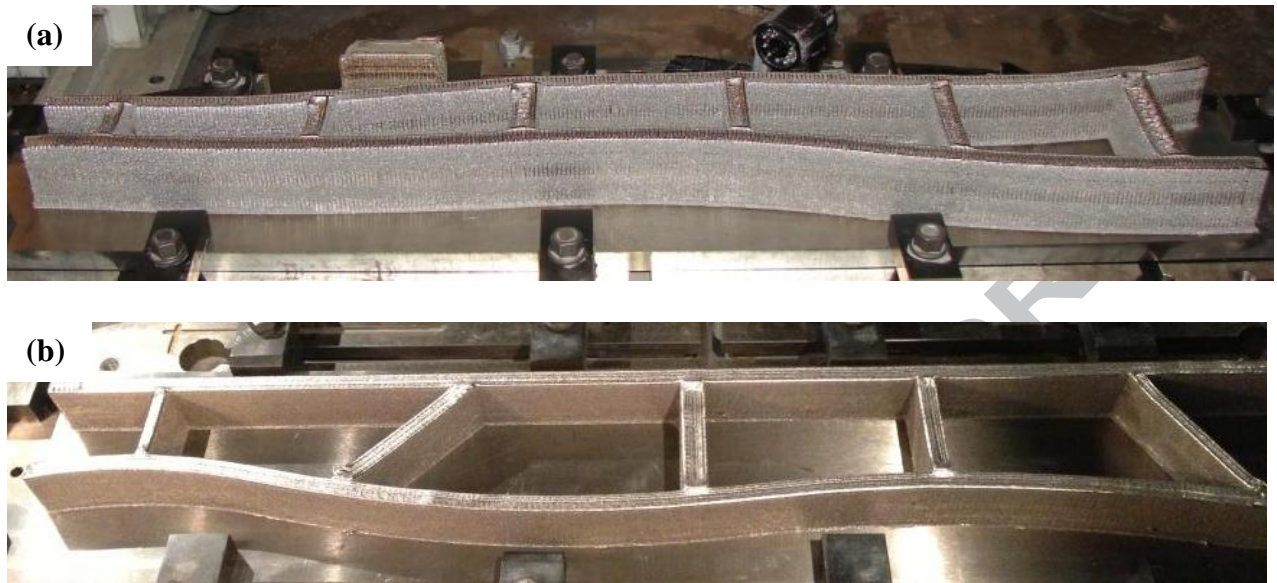


**Fig. 13**

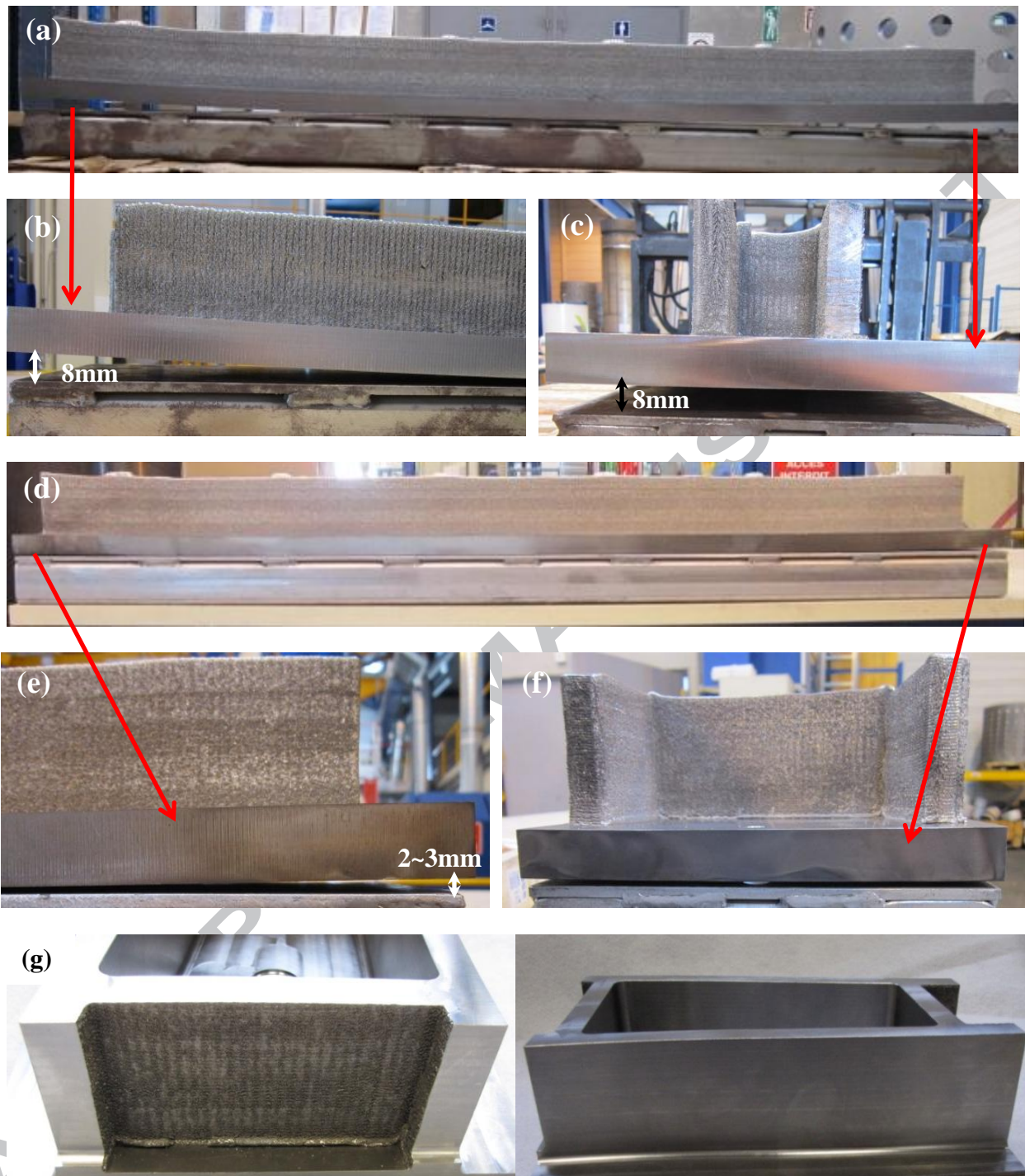
**Fig. 14**

Table 1 DLD Process conditions that give rise to required geometry and build height

Good Process conditions	Laser power (W)	Scanning speed (mm/min)	Powder feed rate (g/min)	Z step (mm)
Process 1	$(P_o+290)$	$(S_p-115)$	$f_o+8.5$	$Z_o+0.85$
Process 2	$P_o$	$S_p$	$f_o$	$Z_o$
Process 3	$(P_o+115)$	$S_p$	$f_o$	$Z_o+0.05$
Process 4	$(P_o+260)$	$S_p$	$f_o+0.5\sim 1.0$	$Z_o+0.13$

$P_o$  is a laser power between 1100-1200W,  $S_p$  is a laser scanning speed between 750- 850mm/min,  $f_o$  is a powder feed rate between 6.5-7.5g/min and  $Z_o=0.71$ mm

Table 2 Build status of samples with different sizes and dimensions after deposition with different Z steps but with some processing condition

Sample geometry $a*b*c$ (mm)	Z step	Build status
111*75*10	$Z_o+0.133$	Under build
	$Z_o+0.12$	Good build
111*75*22	$Z_o+0.091$	Under build
	$Z_o$	Good build
160*140*18	$Z_o+0.12$	Under build
	$Z_o+0.085$	Good build
328*85*18	$Z_o+0.085$	Under build
	$Z_o+0.063$	Good build

Table 3 Tensile properties of as-DLDed and DLDed+HIPed Ti-6Al-4V samples in comparison with tensile data of forged and heat treated samples.

Processing condition	0.2% yield strength (MPa)	UTS (MPa)	Elongation (%)
As-DLDed vertical	950±2	1025±2	5±1
As-DLDed horizontal	950±2	1025±10	12±1
DLDed+HIPed	850±2	920±1	17±2
Forged + heat treated [18]	878±4	926±2	20±1

### Highlights

- High laser power and a reasonably low powder feed rate are key to low porosity
- Scaling-up of samples requires smaller Z steps to achieve geometrical integrity
- HIPing effectively closed pores, changed microstructure and improved ductility
- Optimised processing conditions plus HIPing led to good quality Ti-64 structures
- HIPing helps recover shape of unclamped large structures from distortion